

# $^{81}\text{Br}$ Nuclear Quadrupole Relaxation in Aluminium Tribromide

Noriaki Okubo, Mutsuo Igarashi\*, and Ryozyo Yoshizaki\*\*

Institute of Physics, University of Tsukuba, Tsukuba, 305 Japan

\* Department of Applied Physics, Gunma College of Technology Maebashi, 371 Japan

\*\* Institute of Applied Physics, University of Tsukuba, Tsukuba, 305 Japan

Z. Naturforsch. **50a**, 737–741 (1995); received February 20, 1995

The  $^{81}\text{Br}$  nuclear spin-lattice relaxation time in  $\text{AlBr}_3$  has been measured between 8 K and room temperature. The result is analyzed using the theory of the Raman process based on covalency. A Debye temperature of 67.6 K and covalency of 0.070 and 0.072 for terminal and 0.022 for bridging bonds are obtained. The correspondence of the latter values to those obtained from the NQR frequencies is low, in contrast to the previously examined compounds.

**Key words:** Aluminium tribromide; Nuclear quadrupole relaxation; Raman process; Debye temperature; Covalency.

## 1. Introduction

In the preceding papers [1, 2] we showed that spin-lattice relaxation in the halogen NQR of a few compounds can be explained by the theory of the Raman process based on covalency [3]. In order to extend the application of this theory,  $^{81}\text{Br}$  nuclear relaxation in aluminium tribromide ( $\text{AlBr}_3$ ) has been examined.

The crystal structure of  $\text{AlBr}_3$  is monoclinic, space group  $P2_1/a$  [4]. Though the Br atoms are by themselves in a slightly deformed hexagonal close packing throughout the crystal, there apparently exist dimeric molecules  $\text{Al}_2\text{Br}_6$ . As shown in Fig. 1, the Al atom is surrounded by a tetrahedron of Br atoms, and the dimer consists of two tetrahedra sharing one edge.

For  $\text{AlBr}_3$  both the aluminium and the bromine NQR are reported [5–8]. However, unlike the relaxation of  $^{79}\text{Br}$  and  $^{81}\text{Br}$  nuclei (both spin  $I = 3/2$ ), that

of  $^{27}\text{Al}$  nuclei ( $I = 5/2$ ) is governed by two relaxation times, and it is not easy to determine them separately. Moreover, the Al atom is bonded to nonequivalent Br atoms in the  $\text{Al}_2\text{Br}_6$  dimer, whereas the theory assumes equivalency of the partner atoms. Since the resonance frequencies of Al and Br nuclei differ much, there is no interaction between their relaxation. This paper treats only the bromine nuclear relaxation.

## 2. Experimental

$\text{AlBr}_3$  (Wako Pure Chemicals) of purity higher than 99% was used without further purification. About 5 g of  $\text{AlBr}_3$  were sealed in a pyrex ampoule with a small amount of helium gas, and then the sample was melted and annealed.

The  $^{79}\text{Br}$  and  $^{81}\text{Br}$  NQR were observed with a pulse spectrometer (Matec Inc.). The spin echo signal after  $90^\circ$ – $180^\circ$  pulses was monitored. The signal-to-noise ratio of the  $^{81}\text{Br}$  nuclei for the three sites was nearly equal, namely 30 at 77 K, after 64 times averaging.  $T_1$  was determined by measuring the echo height  $S(t)$  at time  $t$  after saturation by another  $90^\circ$  pulse. The recovery curve could be fitted with a single exponential function within experimental errors.

## 3. Results

The  $^{81}\text{Br}$  NQR spectrum consists of three lines of about 81.8 MHz ( $\nu_1$ ), 95.0 MHz ( $\nu_2$ ), and 96.4 MHz

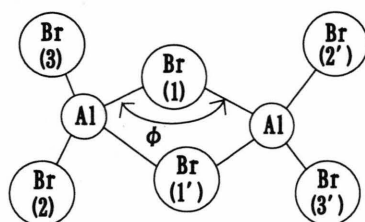


Fig. 1. Dimeric molecule  $\text{Al}_2\text{Br}_6$  in the crystal of  $\text{AlBr}_3$ . Br(1) represents the bridging atom and Br(2) and Br(3) the terminal ones.

Reprint requests to Dr. N. Okubo.

0932-0784 / 95 / 0800-0737 \$ 06.00 © – Verlag der Zeitschrift für Naturforschung, D-72027 Tübingen



Dieses Werk wurde im Jahr 2013 vom Verlag Zeitschrift für Naturforschung in Zusammenarbeit mit der Max-Planck-Gesellschaft zur Förderung der Wissenschaften e.V. digitalisiert und unter folgender Lizenz veröffentlicht: Creative Commons Namensnennung-Keine Bearbeitung 3.0 Deutschland Lizenz.

Zum 01.01.2015 ist eine Anpassung der Lizenzbedingungen (Entfall der Creative Commons Lizenzbedingung „Keine Bearbeitung“) beabsichtigt, um eine Nachnutzung auch im Rahmen zukünftiger wissenschaftlicher Nutzungsformen zu ermöglichen.

This work has been digitalized and published in 2013 by Verlag Zeitschrift für Naturforschung in cooperation with the Max Planck Society for the Advancement of Science under a Creative Commons Attribution-NoDerivs 3.0 Germany License.

On 01.01.2015 it is planned to change the License Conditions (the removal of the Creative Commons License condition “no derivative works”). This is to allow reuse in the area of future scientific usage.

( $\nu_3$ ) at 77 K [5, 8].  $\nu_1$  is assigned to the bridging (Br(1)), and  $\nu_2$  and  $\nu_3$  to the terminal (Br(2) and Br(3)) atoms, respectively [7].

Our values of the resonance frequencies above 77 K agreed with the reported ones [8]. The values below 77 K were also on the extrapolated curves and the values at 4.2 K were 82.142, 95.520, and 96.966 MHz, respectively, with errors of  $\pm 0.004$  MHz.

Figure 2 shows the temperature dependence of  $T_1$  ( $^{81}\text{Br}$ ) for the three lines. Though at 4.2 K the  $T_1$ 's were too long to be measured exactly, they were estimated to be  $10^3$  s. This indicates that the values of  $T_1$  are intrinsic and not shortened by magnetic impurities down to such low temperatures. As the temperature increases, the slope in the log-log plot becomes progressively gentler and approaches  $-2$ . The signal could also be observed above room temperature, but the error in  $T_1$  became large because the separation between the  $90^\circ$  and  $180^\circ$  pulses (typically 200  $\mu\text{s}$ ) could not be neglected for the measurement of such short  $T_1$ .

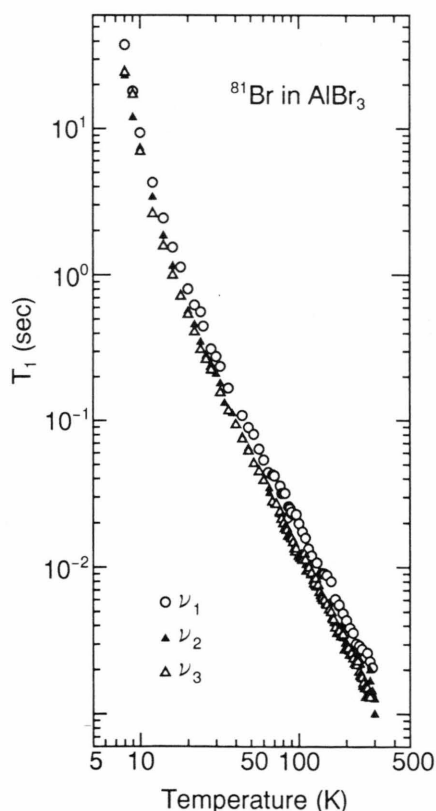


Fig. 2. Temperature dependence of  $T_1$  for the three  $^{81}\text{Br}$  NQR lines in  $\text{AlBr}_3$ .

The ratio  $T_1(^{81}\text{Br})^{-1}/T_1(^{79}\text{Br})^{-1}$  was  $0.65 \pm 0.05$  for the three sites at 77 K. This is close to the squared ratio of the quadrupole moments  $Q$ ,  $[Q(^{81}\text{Br})/Q(^{79}\text{Br})]^2 = 0.6978$  rather than that of the magnetic moments  $\mu$ ,  $[\mu(^{81}\text{Br})/\mu(^{79}\text{Br})]^2 = 1.1618$ . Therefore, the relaxation can be attributed mainly to the quadrupolar interaction.

Both  $T_2$  and  $T_2^*$  were nearly equal among the three sites, and  $T_2$  was  $0.30 \pm 0.01$  ms and  $T_2^*$  was  $70 \pm 10$   $\mu\text{s}$  for  $^{81}\text{Br}$  nuclei typically at 77 K.

## 4. Analysis and Discussion

### 4.1 Raman Process

The approach of  $T_1^{-1}$  to a  $T^2$  dependence with increasing temperature suggests that the relaxation is dominated by the Raman process.

For  $I = 3/2$ ,  $T_1^{-1}$  due to this process is given by [9]

$$T_1^{-1} = \frac{3e^4 Q^2 \langle r^{-3} \rangle_H^2 c^3}{100 \pi^3 a^7 d^2 v_s^3} \cdot T^{*2} \sum_{v=1}^6 (N_{1v} + 4N_{2v}) D_v(T^*), \quad (1)$$

where  $a$  denotes the equilibrium distance from the halogen ion to the metal ion,  $d$  the density of the crystal,  $T^*$  the temperature reduced by the Debye temperature  $\theta_D$ , and  $r$  the interionic distance.  $\langle \rangle_H$  means the expectation value with respect to the valence  $p$  electron of halogen ions.  $c$  is defined as  $c = k_D a$  with the maximum wave number  $k_D = (6\pi^2 N/V)^{1/3}$ ,  $N$  being the number of atoms in the unit cell of volume  $V$ . The sound velocity  $v_s$  is related to  $\theta_D$  by

$$\hbar \omega_D = \hbar v_s k_D = k_B \theta_D, \quad (2)$$

where  $\omega_D$  is the Debye frequency and  $k_B$  the Boltzmann constant.

With the measure of covalency,  $\lambda$ , and its first and second derivatives with respect to  $r$ ,  $\lambda'$  and  $\lambda''$ ,  $N_{\mu\nu}$  for terminal atoms is given by

$$\begin{aligned} N_{11} &= N_{12} = N_{13} = 4\lambda^2 \left( 1 - \frac{a\lambda'}{\lambda} \right)^2, \\ N_{14} &= N_{15} = N_{16} = 0, \\ N_{21} &= N_{22} = N_{23} = \lambda^2, \\ N_{24} &= N_{25} = N_{26} = 0, \end{aligned} \quad (3)$$

and for bridging atoms

$$N_{11} = N_{12} = N_{13} = 8\lambda^2 \left[ 1 - \frac{a\lambda'}{\lambda} + \frac{1}{2} \left( \frac{a\lambda'}{\lambda} \right)^2 \right],$$

$$N_{14} = N_{15} = N_{16} = 8\lambda^2 \left[ (-1 + 2\cos^2\phi) + \left( \frac{a\lambda'}{\lambda} \right) (1 - 2\cos^2\phi) + \frac{1}{2} \left( \frac{a\lambda'}{\lambda} \right)^2 \cos^2\phi \right],$$

$$N_{21} = N_{22} = N_{23}$$

$$= \lambda^2 \left[ \frac{7}{2} - \frac{7}{2} \left( \frac{a\lambda'}{\lambda} \right) + \frac{5}{4} \left( \frac{a\lambda'}{\lambda} \right)^2 + \frac{1}{8} \left( \frac{a^2\lambda''}{\lambda} \right)^2 \right],$$

$$N_{24} = N_{25} = N_{26}$$

$$= \lambda^2 \left[ \left( \frac{1}{2} - 13\cos^2\phi + 16\cos^4\phi \right) + \left( \frac{a\lambda'}{\lambda} \right) \left( \frac{3}{-2} + 18\cos^2\phi - 20\cos^4\phi \right) + \left( \frac{a\lambda'}{\lambda} \right)^2 \left( \frac{7}{8} - \frac{47}{8}\cos^2\phi + \frac{25}{4}\cos^4\phi \right) + \left( \frac{a^2\lambda''}{\lambda} \right) (1 - 5\cos^2\phi + 4\cos^4\phi) + \left( \frac{a\lambda'}{\lambda} \right) \left( \frac{a^2\lambda''}{\lambda} \right) \left( -\frac{1}{4} + \frac{11}{4}\cos^2\phi - \frac{5}{2}\cos^4\phi \right) + \left( \frac{a^2\lambda''}{\lambda} \right)^2 \left( -\frac{1}{8}\cos^2\phi + \frac{1}{4}\cos^4\phi \right) \right], \quad (4)$$

where  $\phi$  denotes the angle between the bridging bonds, cf. Figure 1.

$D_v(T^*)$  is defined as

$$D_v(T^*) = T^* \int_0^{1/T^*} \frac{x^2 e^x}{(e^x - 1)^2} L_v(c T^* x) dx, \quad (5)$$

where  $x = \hbar\omega/k_B T$ ,  $\omega$  being the angular frequency of the phonons.  $L_v(c T^* x) = L_v(k a)$  generally has the following forms:

$$L_1(k a) = \{S_1^2\}_k^2 = [\tfrac{1}{2} - \tfrac{1}{2}f(2ka)]^2,$$

$$L_2(k a) = \{C_1^2\}_k^2 = [\tfrac{3}{2} - 2f(ka) + \tfrac{1}{2}f(2ka)]^2,$$

$$L_3(k a) = 2\{S_1^2 C_1^2\}_k = 2[\tfrac{1}{2} - \tfrac{1}{2}f(2ka)][\tfrac{3}{2} - 2f(ka) + \tfrac{1}{2}f(2ka)],$$

$$L_4(k a) = \{S_1 S_2\}_k^2 = [-\tfrac{1}{2}f(\sqrt{2(1+\cos\phi)}ka) + \tfrac{1}{2}f(\sqrt{2(1-\cos\phi)}ka)]^2,$$

$$L_5(k a) = \{C_1 C_2\}_k^2 = [1 - 2f(ka) + \tfrac{1}{2}f(\sqrt{2(1+\cos\phi)}ka) + \tfrac{1}{2}f(\sqrt{2(1-\cos\phi)}ka)]^2,$$

$$L_6(k a) = 2\{S_1 S_2 C_1 C_2\}_k = 2[-\tfrac{1}{2}f(\sqrt{2(1+\cos\phi)}ka) + \tfrac{1}{2}f(\sqrt{2(1-\cos\phi)}ka)][1 - 2f(ka) + \tfrac{1}{2}f(\sqrt{2(1+\cos\phi)}ka) + \tfrac{1}{2}f(\sqrt{2(1-\cos\phi)}ka)], \quad (6)$$

where

$$S_n = \sin(a\mathbf{k} \cdot \mathbf{n}), \quad C_n = \cos(a\mathbf{k} \cdot \mathbf{n}) - 1, \quad f(y) = \frac{\sin y}{y}, \quad (7)$$

and  $\{\}_k$  means the average about the direction of  $\mathbf{k}$ ,  $\mathbf{k}$  being the wave vector of the phonon,  $k$  its magnitude and  $\mathbf{n}$  the unit vector from the halogen ion to the metal one.

#### 4.2 Estimation of Debye Temperature

Introducing a scaling time  $\tau$  defined as

$$\tau^{-1} = \frac{3e^4 Q^2 \langle r^{-3} \rangle_{\text{H}}^2 c^3}{100\pi^3 a^7 d^2 v_s^3} (N_{11} + 4N_{21}), \quad (8)$$

(1) can be reduced to a form convenient for fitting:

$$(T_1 T^2)^{-1} = (\tau \theta_D^2)^{-1} \cdot \left[ \sum_{v=1}^3 D_v(T^*) + \varepsilon \sum_{v=4}^6 D_v(T^*) \right] \quad (9)$$

where

$$\varepsilon = \frac{N_{14} + 4N_{24}}{N_{11} + 4N_{21}}. \quad (10)$$

For terminal atoms  $\varepsilon$  vanishes, while for bridging ones  $\varepsilon$  is calculated to be 0.3067 by using  $\phi$  in Table 1. Then, by fitting (9) to the experimental result, we can determine  $\theta_D$  together with  $\tau$  as fitting parameters. The integration in (5) was carried out numerically. Table 2 and Fig. 3 show the results of a least-squares-fitting performed for the data 8 K to 200 K with an assumption of a common  $\theta_D$  for three sites. Then, by means of (2), we obtain  $v_s = 7.33 \times 10^4$  cm/sec. Even when the fitting is made for the data up to 250 K or with an assumption of separate  $\theta_D$ 's for the three sites, the obtained  $\theta_D$ 's differ by only a few degrees from the above value.

Table 1. Crystal data [4].

$N$	$V$ ( $\text{\AA}^3$ )	$a$ ( $\text{\AA}$ )	$\phi$ (degree) [6]
16	538.0	$\left. \begin{array}{l} 2.34 \text{ (Br(1))} \\ 2.42 \text{ (Br(1'))} \\ 2.33 \text{ (Br(2))} \\ 2.23 \text{ (Br(3))} \end{array} \right\}$	82

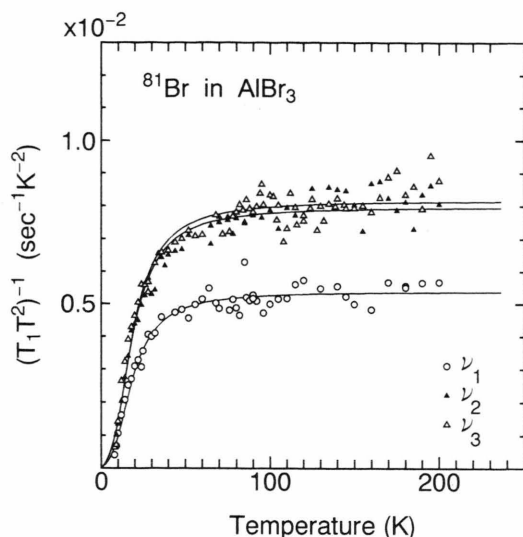


Fig. 3. The result of a least-squares-fitting of (9) to the data for the three NQR lines in  $\text{AlBr}_3$ .

Table 2. Debye temperature  $\theta_D$  and scaling time  $\tau$ .

Site	$\theta_D$ (K)	$\tau$ (s)
Br(1)	67.6	0.0355
Br(2)		0.0219
Br(3)		0.0188

#### 4.3 Estimation of Covalency

Now we can estimate  $\lambda$  from  $\tau$  using (8), with (3) or (4). The  $e^2 Q \langle r^{-3} \rangle_H$  is given by  $(5/4) e^2 Q q_{\text{at}}$ ,  $e^2 Q q_{\text{at}}$  being the quadrupole coupling constant for the free atom, which is reported to be 643.033 MHz for  $^{81}\text{Br}$  [10].  $c = k_D a$  is calculated to be 2.874 as an average for Br(1), 2.814 for Br(2), and 2.693 for Br(3) from the data in Table 1. The relation

$$\lambda \propto \exp(-r/\rho) \quad (11)$$

and a value of 0.345 Å for the repulsive range parameter  $\rho$  were assumed as before [1–3]. Thus we obtain the values of  $\lambda$  in Table 3. In the table the results for the previously examined compounds [9] are listed for comparison.

$\lambda$  is defined as the amount of  $p$  electrons which is transferred from the halogen ion to the metal ion in forming covalent bonding and is supposed to produce the EFG with the largest component along the bond [3]. It just corresponds to the number of unbalanced  $p$

electrons,  $f$ , defined as [11]

$$f = \frac{e^2 Q q_{\text{mol}}}{e^2 Q q_{\text{at}}}, \quad (12)$$

where  $e^2 Q q_{\text{mol}}$  is the coupling constant for the molecule and related with the resonance frequency  $\nu_Q$  by

$$\nu_Q = \frac{e^2 Q q_{\text{mol}}}{2h} (1 + \eta^2/3)^{1/2}. \quad (13)$$

Here  $\eta$  denotes the asymmetry parameter, whose value is reported to be 0.248 for Br(1), 0.073 for Br(2), and 0.106 for Br(3) in  $\text{AlBr}_3$  at 77 K [7]. Thus we can compare  $\lambda$  determined from  $T_1$  with  $f$  determined independently from  $\nu_Q$ . The thermal effect involved in  $\nu_Q$  was removed by using the values at 0 K extrapolated from  $\nu_Q(T)$  at higher temperatures. Then we obtain the values of  $f$  in Table 3.

#### 4.4 Concluding Remarks

The ratio  $\lambda/f$  for  $\text{AlBr}_3$  is significantly smaller than those for the previously examined compounds. Rather large  $\eta$ 's for terminal atoms suggest the existence of intermolecular bondings [7]. However, even if intermolecular bonding is assumed between these Br atoms and the corresponding nearest Al atoms, and if an analysis similar to the case of  $\text{SbCl}_3$  [2] is made, the change in  $f$  does not exceed 10%. When  $\theta_D$  is low, the anharmonic Raman process is expected to become effective, but inclusion of the contribution to  $T_1^{-1}$  makes the estimated  $\lambda$  even smaller. Though neither

Table 3. The two measures of covalency,  $\lambda$  and  $f$ .

Compound	Site	$\lambda^a$	$f^b$	$\lambda/f$
$\text{AlBr}_3$	Br(1)	0.022	0.256	0.086
	Br(2)	0.070	0.303	0.231
	Br(3)	0.072	0.306	0.235
$\text{SbCl}_3$	Cl(I)	0.284	0.387	0.734
	Cl(II)	0.260	0.355	0.732
$\text{NbCl}_5$	Cl(br)	0.039	0.245	0.159
	Cl(eq)	0.096	0.133	0.722
	Cl(ax)	0.107	0.132	0.811
$\text{NbBr}_5$	Br(br)	0.025	0.283	0.088
	Br(eq)	0.075	0.153	0.490
	Br(ax)	0.075	0.152	0.493

<sup>a</sup> Corrected for the lack of inversion symmetry also in the other compounds.

<sup>b</sup> Corrected for thermal effect but, as for niobium compounds, still with the assumption  $\eta=0$ .

the value of  $\theta_D$  nor the temperature factor in the X-ray analysis is reported,  $\theta_D$  of 67.6 K seems to be fairly low compared with  $\theta_D$ 's of other compounds. Also in  $\text{NbBr}_5$ , exhibiting low  $\theta_D$ , the agreement between  $\lambda$  and  $f$  is small. According to (1), for a given  $T_1^{-1}$ ,  $\lambda$  depends on  $\theta_D$  more strongly than  $\theta_D^{5/2}$ . Correspondingly, when  $\theta_D$  is estimated to be smaller than the actual value,  $\lambda$  is also estimated to be smaller than otherwise. As a conclusion, we may say that, as the Debye temperature becomes lower, the difference between the Debye model and the actual phonon spec-

trum is reflected more strikingly in  $\lambda$  through the strong dependence of  $\lambda$  on  $\theta_D$ .

As in niobium halides, it is also observed in  $\text{AlBr}_3$  that  $\lambda/f$  for bridging atoms is much smaller than that for terminal ones, but the difference is smaller in  $\text{AlBr}_3$ . This may be attributed the fact that the fraction of the number of bridging atoms in the unit cell is larger in this compound. In the present treatment, assuming equivalence of the ions, this is expected to bring about a raising of  $\lambda/f$  for bridging atoms at the expense of the lowering of it for terminal ones.

- [1] N. Okubo, H. Sekiya, C. Ishikawa, and Y. Abe, *Z. Naturforsch.* **47a**, 713 (1992).
- [2] N. Okubo and Y. Abe, *Z. Naturforsch.* **49a**, 680 (1994).
- [3] K. Yosida and Y. Moriya, *J. Phys. Soc. Japan* **11**, 33 (1956).
- [4] P. A. Renes and C. H. MacGillavry, *Rec. Trav. Chim.* **64**, 275 (1945).
- [5] R. G. Barnes and S. L. Segel, *J. Chem. Phys.* **25**, 180 (1956).
- [6] P. A. Casabella, P. J. Bray, and R. G. Barnes, *J. Chem. Phys.* **30**, 1393 (1959).
- [7] T. Okuda, H. Terao, O. Ege, and H. Negita, *J. Chem. Phys.* **52**, 5489 (1970).
- [8] N. Weiden and A. Weiss, *J. Mag. Res.* **20**, 334 (1975).
- [9] In the summation of (4.26) in [3], terms with  $s=s'$  do not vanish for the case where inversion symmetry about the nucleus in problem is lacking. In [1, 2] these terms were missed. Leaving these terms, we have the present  $L_3$  and  $L_6$  in (6). In (1), (3), (4), (6), (9), and (10) the corresponding modifications have been made and the corrected results for the previously examined compounds are listed in Table 3.
- [10] J. G. King and V. Jaccarino, *Phys. Rev.* **94**, 1610 (1954).
- [11] In [1],  $\lambda$  for bridging atoms was compared with half the value obtained from (12), because in the approximation of the bond angle as  $90^\circ$ , the EFG along each bond is half that along the principal axis perpendicular to the bonds, after averaging due to bond switching. However, according to (4.6) of [3],  $\lambda$  corresponds to the EFG for each bond before the summation, so that it should be still compared with  $f$  itself also at bridging atoms.